HOSTED BY

ELSEVIER

Available online at www.sciencedirect.com

ScienceDirect

journal homepage: www.elsevier.com/locate/bjbas

Full Length Article

# Evaluation of optimum adsorption conditions for Ni (II) and Cd (II) removal from aqueous solution by modified plantain peels (MPP)

*Zaharaddeen N. Garba* [a,b,*], *Nkole I. Ugbaga* [b], *Amina K. Abdullahi* [b]

[a] *School of Chemical Sciences, Universiti Sains Malaysia, 11800 Penang, Malaysia*
[b] *Department of Chemistry, Ahmadu Bello University, P.M.B., 1044 Zaria, Nigeria*

ARTICLE INFO

*Article history:*
Received 11 December 2015
Received in revised form 18 March 2016
Accepted 20 March 2016
Available online 1 June 2016

*Keywords:*
Modified plantain peel (MPP)
Adsorption
Central composite design (CCD)
Response surface methodology (RSM)
Ni (II) and Cd (II)

ABSTRACT

The most ideal conditions for the adsorption of Ni (II) and Cd (II) ions onto modified plantain peel (MPP) from aqueous solution were investigated. The effects of three adsorption variables (pH, MPP dose and initial adsorbate concentration) were studied using central composite design (CCD), a subset of response surface methodology (RSM). Quadratic models were developed for both Ni (II) and Cd (II) percentage removals. The prime adsorption conditions obtained were pH of 4.36, MPP dose of 0.82 g and initial concentration of 120 mg/L with desirability of 1.00 which gave good monolayer adsorption capacities of 77.52 and 70.92 mg/g for Ni (II) and Cd (II) respectively. The adsorption data were modelled using Langmuir and Freundlich adsorption isotherms; the equilibrium adsorption of both Ni (II) and Cd (II) on MPP obeyed Langmuir model, and pseudo-second-order kinetics was the order that best described the two adsorption processes.

© 2016 Beni-Suef University. Production and hosting by Elsevier B.V. This is an open access article under the CC BY-NC-ND license (http://creativecommons.org/licenses/by-nc-nd/4.0/).

## 1. Introduction

Air, food, soil and water were narrated to be the media where heavy metals such as copper, cadmium, nickel, lead, and zinc are introduced into the environment (Garba et al., 2015c; Sadaf et al., 2015). These heavy metals are reported to be hazardous resulting in damage to ecosystems as well as human health (Ozdes et al., 2009; Tuzen et al., 2009) especially if their concentration is more than the accepted limit (Alslaibi et al., 2013). Their main sources include wastewater discharged from hospitals (Verlicchi et al., 2010), different industries such as Cd–Ni battery, metal plating and alloy manufacturing (Khavidaki and Aghaie, 2013; Kobya et al., 2005; Krishnan et al., 2011; Kula et al., 2008). Presence of these metals in waste stream and ground water is a very serious environmental concern since these metal ions are toxic to various life forms; therefore, removing them as well as controlling their levels in waste waters is very crucial (Serencam et al., 2008).

* *Corresponding author.* School of Chemical Sciences, Universiti Sains Malaysia, 11800 Penang, Malaysia. Tel.: +60 1126116051; fax: +60 46574854.
*E-mail address:* dinigetso2000@gmail.com (Z.N. Garba).
http://dx.doi.org/10.1016/j.bjbas.2016.03.001
2314-8535/© 2016 Beni-Suef University. Production and hosting by Elsevier B.V. This is an open access article under the CC BY-NC-ND license (http://creativecommons.org/licenses/by-nc-nd/4.0/).

Chemical precipitation, ion exchange, electrodialysis, solvent extraction, coagulation, evaporation and adsorption are among the most prevalent technologies for the removal of metal ions from aqueous solutions (Garba and Afidah, 2014; Garba et al., 2014, 2015b; Mohammadi et al., 2015; Mohan et al., 2008; Mondal et al., 2015), with adsorption being the most widely used method for removing contaminants from wastewater (Farghali et al., 2013; Garba et al., 2015a). Sorption methods are considered flexible and easy to operate with much less sludge disposal problems (Cao et al., 2014; Mohammadi et al., 2015).

Various adsorbents were narrated in the literature for the removal of heavy metal ions; however, new adsorbents with local availability, high adsorption capacity as well as economic suitability are still needed. This prompted many researchers into investigating cheaper substitutes such as zeolites, silica gel, chitosan, clay materials and agricultural wastes (Mekatel et al., 2015; Shirzad-Siboni et al., 2015; Tsai et al., 1998). Response surface methodology (RSM) is a mathematical model that was reported to be a very useful tool in optimizing the preparation conditions of activated carbons (Garba and Afidah, 2015), but not much was reported on its application in optimizing adsorption process parameters.

Therefore, the innovative aspect of this research is to optimize the paramount parameters for an effective adsorption of Ni (II) and Cd (II) from an aqueous solution using CCD. CCD was chosen to evaluate the interaction of the most crucial adsorption parameters such as pH, MPP dose as well as initial concentrations.

## 2. Materials and methods

### 2.1. Reagents

All the chemicals used in this work were of analytical reagent grade purchased from Sigma-Aldrich and Merck (Darmstadt, Germany); they were used without any further purification. All the glassware used was washed and rinsed several times. Nickel and cadmium solutions and standards were prepared by using analytical grade nickel chloride ($NiCl_2{\cdot}6H_2O$) and cadmium chloride ($CdCl_2$) with distilled water. The solutions of Ni (II) and Cd (II) were prepared from stock solutions containing 1000 mg/L of Ni (II) and Cd(II), respectively.

### 2.2. Preparation of adsorbent material

Plantain peels used in this study were collected from local food sellers, restaurants and eateries around Samaru and Sabon Gari Local Government of Kaduna state, Nigeria. They were washed and sun dried for 7 days. The dried plantain peels were then crushed into smaller particles in a mortar and sieved with 150 μm sieve until a reasonable quantity of that particle size is obtained, followed by repeated washing to eliminate dust and other impurities. It was then dried in an oven at 25 °C for about 48 h after which it was stored in sterilized closed glass bottles prior to use as an adsorbent. The powdered plantain peels were then modified by immersing in 5% solution of NaOH and autoclaved at 121 °C for 15 min at 10 psi. After keeping at 25 °C for 48 h, it was filtered and washed many times with distilled water until clear water with neutral pH was obtained (Ashrafi et al., 2014). Then, the modified plantain peel (MPP) was dried at 25 °C for 48 h. The MPP was applied for all the adsorption experiments.

### 2.3. Metal ions adsorption experiments

In order to study and evaluate the significance of variables on the percentage removal of Ni (II) and Cd (II), the adsorption experiments were carried out using a batch procedure by shaking 100 mL of the metal ions solutions in a 250 mL Erlenmeyer flask according to the pH, MPP dose and initial concentration as shown in Table 1. The coded points and their corresponding values are presented in Table 2. During the adsorption process, the flasks were agitated on a mechanical shaker at 150 rpm. The aqueous samples were analysed using an inductively coupled plasma-atomic emission spectrometer. The adsorption efficiencies were evaluated using the following equation:

$$\text{Adsorption efficiency}\ (\%) = \frac{C_o - C_e}{C_o} \times 100 \tag{1}$$

where $C_o$ and $C_e$ are the liquid-phase concentrations at initial and equilibrium states (mg/L), respectively.

The equilibrium amounts $q_e$ (mg/g) adsorbed per unit mass of adsorbent were evaluated using Equation (2):

$$q_e = \frac{(C_o - C_e)V}{W} \tag{2}$$

where $q_e$ (mg/g) is the equilibrium amount of the metal ions adsorbed per unit mass of MPP; V (L) is the volume of the solution and W (g) is the mass of MPP used.

The kinetic tests were identical to those of equilibrium. The aqueous samples were taken at preset time intervals and the metal ions concentrations were measured. The amount adsorbed at time t, $q_t$ (mg/g) was calculated using Equation (3):

$$q_t = \frac{(C_o - C_t)V}{W} \tag{3}$$

where $C_o$ and $C_t$ (mg/L) are the liquid-phase concentration at the initial and any time t, respectively.

### 2.4. Adsorption isotherms and kinetic models

#### 2.4.1. Adsorption isotherm

The equilibrium characteristics of this adsorption study were described through Langmuir (Lang) and Freundlich (Freund). Lang model presumes monolayer adsorption onto a surface containing finite number of adsorption sites (Langmuir, 1916). Its linear form is given as:

$$\frac{C_e}{q_e} = \frac{1}{K_L \cdot Q_a^0} + \frac{C_e}{Q_a^0} \tag{4}$$

$Q_a^0$(mg/g) and $K_L$ (L/mg) are Lang constants related to adsorption capacity and rate of adsorption, respectively.

The essential characteristics of Lang model can be described by dimensionless separation factor, $R_L$, given as:

**Table 1 – Experimental design matrix using central composite design.**

| Run | Level | | | Ni (II) and Cd (II) adsorption variables | | | Ni (II) removal | Cd (II) removal |
|---|---|---|---|---|---|---|---|---|
| | | | | pH | Adsorbent dosage (g) | Initial concentration (mg/L) | $Y_{Ni}$ (%) | $Y_{Cd}$ (%) |
| 1 | −1 | −1 | −1 | 4.00 | 0.30 | 50 | 42.73 | 24.27 |
| 2 | +1 | −1 | −1 | 10.00 | 0.30 | 50 | 44.67 | 21.16 |
| 3 | −1 | +1 | −1 | 4.00 | 0.80 | 50 | 94.28 | 96.71 |
| 4 | +1 | +1 | −1 | 10.00 | 0.80 | 50 | 89.64 | 57.57 |
| 5 | −1 | −1 | +1 | 4.00 | 0.30 | 125 | 42.88 | 37.38 |
| 6 | +1 | −1 | +1 | 10.00 | 0.30 | 125 | 40.63 | 13.93 |
| 7 | −1 | +1 | +1 | 4.00 | 0.80 | 125 | 99.04 | 98.80 |
| 8 | +1 | +1 | +1 | 10.00 | 0.80 | 125 | 99.79 | 48.30 |
| 9 | −1.682 | 0 | 0 | 2.00 | 0.60 | 88 | 65.53 | 99.43 |
| 10 | +1.682 | 0 | 0 | 12.00 | 0.60 | 88 | 34.68 | 10.44 |
| 11 | 0 | −1.682 | 0 | 7.00 | 0.10 | 88 | 22.46 | 17.76 |
| 12 | 0 | +1.682 | 0 | 7.00 | 1.00 | 88 | 92.35 | 98.55 |
| 13 | 0 | 0 | −1.682 | 7.00 | 0.60 | 25 | 61.07 | 89.77 |
| 14 | 0 | 0 | +1.682 | 7.00 | 0.60 | 150 | 73.48 | 98.82 |
| 15 | 0 | 0 | 0 | 7.00 | 0.60 | 88 | 76.71 | 82.65 |
| 16 | 0 | 0 | 0 | 7.00 | 0.60 | 88 | 83.12 | 79.66 |
| 17 | 0 | 0 | 0 | 7.00 | 0.60 | 88 | 79.15 | 85.11 |
| 18 | 0 | 0 | 0 | 7.00 | 0.60 | 88 | 85.61 | 82.31 |
| 19 | 0 | 0 | 0 | 7.00 | 0.60 | 88 | 81.07 | 83.32 |
| 20 | 0 | 0 | 0 | 7.00 | 0.60 | 88 | 85.72 | 85.14 |

$$R_L = \frac{1}{1 + K_L C_o} \tag{5}$$

where $C_o$ is the highest initial solute concentration. $R_L$ values indicate whether the adsorption is unfavourable ($R_L > 1$), linear ($R_L = 1$), favourable ($0 < R_L < 1$), or irreversible ($R_L = 0$).

Freund model on the other hand assumes heterogeneous surface energies. Its linear form is given by the following equation (Freundlich, 1906):

$$\log q_e = \log K_F + \frac{1}{n} \log C_e \tag{6}$$

where $K_F$ and n are Freund constants. Generally, $n > 1$ suggests favourable adsorption. It has also been used to evaluate whether the adsorption process is physical ($n > 1$), chemical ($n < 1$) or linear ($n = 1$) (Martins et al., 2015).

### 2.4.2. *Kinetic models*

The kinetic data were fitted using the pseudo-first-order and pseudo-second-order models. The rate constant of adsorption is determined from the pseudo-first-order equation given as (Lagergren and Svenska, 1898):

$$\log(q_e - q_t) = \log q_e - \frac{k_1}{2.303} t \tag{7}$$

where $q_e$ and $q_t$ are the amount of metal ions adsorbed (mg/g) at equilibrium and at time t (h), respectively while $k_1$ is the adsorption rate constant ($h^{-1}$). The pseudo-second-order equation based on equilibrium adsorption is expressed as (Ho and Mckay, 1998):

$$\frac{t}{q_t} = \frac{1}{k_2 q_e^2} + \frac{1}{q_e} t \tag{8}$$

where $k_2$ (g/mgh) is the rate constant of second-order adsorption.

As the pseudo-first-order and pseudo-second-order kinetic models could not identify the sorption mechanism, the kinetic results were further analysed for the diffusion mechanism by applying the intraparticle diffusion model. The intraparticle diffusion equation is expressed as (Weber and Morris, 1963):

$$q_t = k_{ip} t^{0.5} + C \tag{9}$$

where $k_{ip}$ is rate constant of the intra-particle diffusion equation and C gives information about the boundary layer thickness: larger value of C is associated with the boundary layer diffusion effect. If the adsorption process follows the intraparticle diffusion model, then $q_t$ versus $t^{0.5}$ will be linear; if the plot passes through the origin, then intraparticle diffusion is the sole rate limiting step. Otherwise, some other mechanism along with intraparticle diffusion is also involved (Tan et al., 2009).

**Table 2 – Independent variables and their coded levels using central composite design.**

| Variables | Code | Unit | Coded variable levels | | | | |
|---|---|---|---|---|---|---|---|
| | | | −α | −1 | 0 | +1 | +α |
| pH | $x_1$ | – | 2 | 4 | 7 | 10 | 12 |
| Adsorbent dosage | $x_2$ | g | 0.10 | 0.30 | 0.6 | 0.80 | 1.00 |
| Initial concentration | $x_3$ | mg/L | 25 | 50 | 88 | 125 | 150 |

### 2.5. *Design of experiments using response surface methodology (RSM)*

In this work, a standard RSM design known as central composite design (CCD) was applied to study the Ni (II) and Cd (II) adsorption parameters (pH, MPP dose and initial adsorbate concentrations). The detailed CCD process was described in our previously published paper (Garba and Afidah, 2014). Design expert statistical software (version 6.0.8, Stat-Ease, Inc., Minneapolis, MN, USA) was used for the model fitting and significance for the Ni (II) and Cd (II) adsorption efficiencies.

## 3. Results and discussion

### 3.1. *Development of regression model equations using CCD*

The design matrix comprising the preparation variables, their ranges and the responses ($Y_{Ni}$ and $Y_{Cd}$) respectively were displayed in Table 2. In order to compare and correlate the responses, CCD was applied for the development of the polynomial regression equations which were all quadratic expressions as suggested by the software. The model expression was selected in accordance with sequential model sum of square that is based on the polynomial's highest order where the model was not aliased and the additional terms were significant (Sahu et al., 2010).

The correlation between predicted and experimental data was blatant as shown by the model's $R^2$ values of 0.9448 for Ni (II) and 0.9383 for Cd (II) which were within desirability range (Gómez Pacheco et al., 2012). The final empirical model's equations for percentage removal of both Ni (II) ($Y_{Ni}$) and Cd (II) ($Y_{Cd}$) responses are given as Equations 10 and 11 respectively.

$$Y_{Ni} = 86.37 + 8.31x_1 + 9.84x_2 + 9.96x_3 - 1.37x_1^2 - 3.65x_2^2 - 4.79x_3^2 - 6.64x_1x_2 - 5.76x_1x_3 - 4.62x_2x_3 \quad (10)$$

$$Y_{Cd} = 83.96 + 9.24x_1 + 15.51x_2 + 3.21x_3 - 0.28x_1^2 - 7.30x_2^2 + 0.90x_3^2 - 11.95x_1x_2 - 3.37x_1x_3 - 6.06x_2x_3 \quad (11)$$

The positive and negative signs before the terms indicate synergetic and antagonistic effect of the respective variables (Garba and Afidah, 2014). The appearance of a single variable in a term signified a uni-factor effect; two variables imply a double factor effect and a second order term of variable appearance indicate the quadratic effect (Ahmad and Alrozi, 2010).

The Ni (II) and Cd (II) percentage removals range from 22.46 to 99.79% and from 10.44 to 99.43% respectively; these can be found on the total experimental design matrix, and the values of the responses obtained are presented in Table 1. Quadratic model was used as selected by the software for the two responses. The six replicate variables at the centre points, run 15–20, were conducted to determine the experimental error and the reproducibility of the data.

### 3.2. *Statistical analysis*

In order to evaluate the individual, interaction as well as quadratic effects of the variables influencing the removal efficiency of both Ni (II) and Cd (II), analysis of variance (ANOVA) was performed. The sum of squares and mean square of each factor, F-value as well as Prob. > F values are shown in Table 3 for both Ni (II) and Cd (II) percentage removals. ANOVA validated the importance and adequacy of the models. From Table 3, dividing the sum of the squares of each of the variation sources, the model and the error variance by the respective degrees of freedom gives the mean square values. The model terms with value of Prob.>F less than 0.05 are considered as significant (Ahmad and Alrozi, 2010).

With respect to Ni (II) percentage removal from Table 3, it can be seen that the model F-value is 19.00 and Prob. > F of <0.0001 signifies the model's significance. The significant model terms were $x_1, x_2, x_3, x_2^2$, $x_3^2, x_1x_2, x_1x_3$ and $x_2x_3$ with only $x_1^2$ insignificant to the response. Still from Table 3, F-value of 16.91 as well as Prob.>F of <0.0001 indicated that the model was also significant. In this case $x_1, x_2, x_2^2, x_1x_2$ and $x_2x_3$ were the significant model terms with the insignificant terms being $x_3, x_1^2, x_3^2$ and $x_2x_3$. From the statistical results obtained, it can be seen that the models were suitable in predicting both Ni (II) and Cd (II) removals within the range of the studied variables. Additionally, Fig. 1(a) and (b) shows the predicted values versus the experimental values for Ni (II) and Cd (II) removals respectively, portraying that the developed models successfully captured the relation between the adsorption process variables and the responses.

### 3.3. *Individual and interaction effects of the variables*

From Table 3, it can be observed that the individual effects inflicted by initial concentration and MPP dose on Ni (II) percentage removal were superior with the highest F-values of 49.61 and 45.03 respectively, whereas pH effect was inferior on this response with F-value of 34.50. The quadratic effect of solution pH was more pronounced with F-value of 12.11 while that of MPP dose and initial concentration were low with F-values of 6.43 and 0.99 respectively. The interaction effects between pH–MPP dose and that of pH–initial concentration were analogous with F-values of 11.67 and 10.08 respectively, while that of interaction between MPP dose–initial concentration was less significant with F-value of 5.66. Fig. 2(a) and (b) showed the 3D response surface plots for the studied variables, with Fig. 2(a) demonstrating the effect of pH and MPP dose with initial concentration fixed at zero level (Co = 88 mg/L), whereas Fig. 2(b) demonstrates the effect of pH and initial concentration with MPP dose fixed at zero level (W = 0.6 g), on the same response ($Y_{Ni}$). From both figures, the percentage Ni removal can be seen to increase with upsurge in all the studied variables. Also from Table 3, the three variables (pH, MPP dose and initial concentrations) had uneven impact on the Cd (II) percentage removal. Initial concentration had the least effect as its F-value was smaller and also its variation did not have a significant effect on the process. The individual factors of pH and MPP dose as well as their interactions had the most significant effect on the Cd (II) adsorption as can be seen by their largest F-values as shown in Table 3. The F-values for pH ($x_1$), MPP dose ($x_2$) and initial concentration ($x_3$) were 27.17, 71.15 and 3.28 respectively. The 3-D surface response analysis of pH and MPP dose interaction effect when the initial concentration was fixed ($C_o$ = 88 mg/L) and that of MPP dose and initial

**Table 3 – The ANOVA for response surface quadratic model of Ni (II) and Cd (II) adsorption by MPP.**

| Source | Sum of squares | Degree of freedom | Mean square | F value | Prob > F |
|---|---|---|---|---|---|
| Ni (II) | | | | | |
| Model | 4666.51 | 9 | 518.50 | 19.00 | <0.0001 |
| $x_1$ | 941.57 | 1 | 941.57 | 34.50 | 0.0002 |
| $x_2$ | 1228.90 | 1 | 1228.90 | 45.03 | <0.0001 |
| $x_3$ | 1353.65 | 1 | 1353.65 | 49.61 | <0.0001 |
| $x_1^2$ | 27.14 | 1 | 27.14 | 0.99 | 0.3421 |
| $x_2^2$ | 175.36 | 1 | 175.36 | 6.43 | 0.0296 |
| $x_3^2$ | 330.50 | 1 | 330.50 | 12.11 | 0.0059 |
| $x_1x_2$ | 318.57 | 1 | 318.57 | 11.67 | 0.0066 |
| $x_1x_3$ | 275.04 | 1 | 275.04 | 10.08 | 0.0099 |
| $x_2x_3$ | 154.32 | 1 | 154.32 | 5.66 | 0.0387 |
| Residual | 272.88 | 10 | 27.29 | – | – |
| Cd (II) | | | | | |
| Model | 6531.18 | 9 | 725.69 | 16.91 | <0.0001 |
| $x_1$ | 1166.43 | 1 | 1166.43 | 27.17 | 0.0004 |
| $x_2$ | 3054.34 | 1 | 3054.34 | 71.15 | <0.0001 |
| $x_3$ | 140.92 | 1 | 140.92 | 3.28 | 0.1001 |
| $x_1^2$ | 1.13 | 1 | 1.13 | 0.026 | 0.8744 |
| $x_2^2$ | 701.75 | 1 | 701.75 | 16.35 | 0.0023 |
| $x_3^2$ | 11.68 | 1 | 11.68 | 0.27 | 0.6133 |
| $x_1x_2$ | 1031.63 | 1 | 1031.63 | 24.03 | 0.0006 |
| $x_1x_3$ | 93.98 | 1 | 93.98 | 2.19 | 0.1698 |
| $x_2x_3$ | 265.52 | 1 | 265.52 | 6.19 | 0.0322 |
| Residual | 429.29 | 10 | 42.93 | – | – |

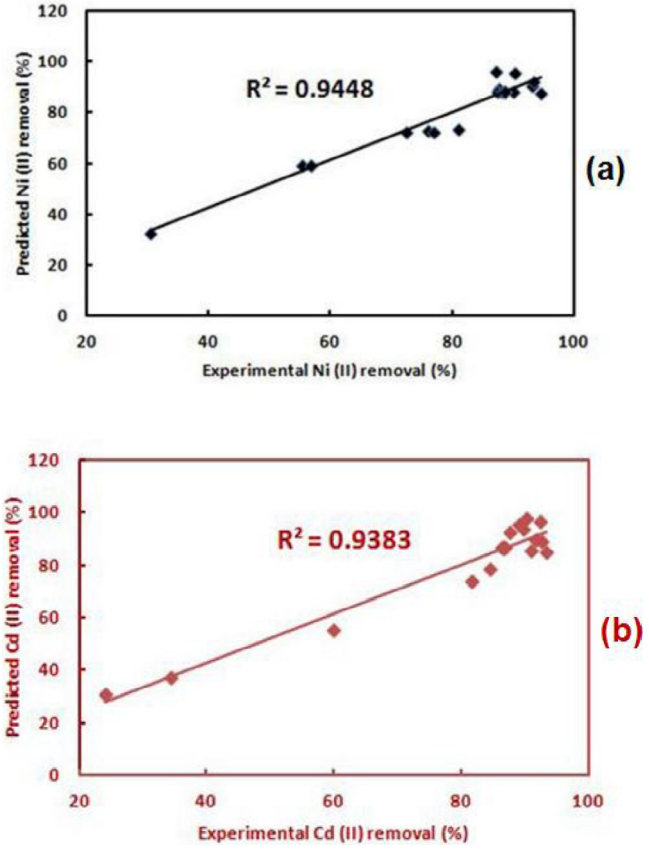


**Fig. 1 – Relationship between predicted and experimental data for (a) Ni (II) removal; for (b) Cd (II) removal.**

concentration when pH was fixed (pH = 7) for Cd (II) adsorption are shown in Fig. 3(a) and (b) respectively. Increase in pH and MPP dose was proportional to high adsorption of Cd (II).

### 3.4. *Process optimization*

The optimization of Ni (II) and Cd (II) adsorption onto MPP was carried out by a multiple response method called the function of desirability, which was applied using design-expert software (Stat-Ease, Inc., Minneapolis, MN, USA). In the optimization analysis, the target criterion was set as maximum values for the two responses. The optimum adsorption conditions obtained were initial concentration of 120 mg/L, MPP dose of 0.82 g at pH of 4.36 with desirability of 1.00. At the optimum conditions, the Ni (II) and Cd (II) removals were found to be 94.88% and 94.82%, respectively. However, the experimental values obtained at optimum conditions for Ni (II) and Cd (II) removals were 93.05% and 94.21% respectively, showing good agreement between the experimental values and those predicted from the models, with relatively small errors which were only 1.83 and 0.61, respectively for Ni (II) and Cd (II) adsorption.

Mohammadi et al. (2015) reported in their work a pH of 5.5 as the optimum pH for the adsorption of Ni (II) and Cd (II) onto dolomite powder, observing the appearance of a metal precipitation at a pH greater than 6 (Mohammadi et al., 2015). Alslaibi et al. (2013) and Subbaiah et al. (2011) also reported optimum pH of 5 in their work of Cd (II) adsorption onto activated carbon from olive stone (Alslaibi et al., 2013) as well as its biosorption by fungus (*Trametes versicolor*) biomass (Subbaiah et al., 2011). Gutha et al. (2015) also observe no appreciable increase in the percentage removal of Ni (II) onto tomato leaf powder at a pH and adsorbent dose greater than 5.5 and 0.4 g respectively, revealing them as the optimum adsorption conditions (Gutha et al., 2015).

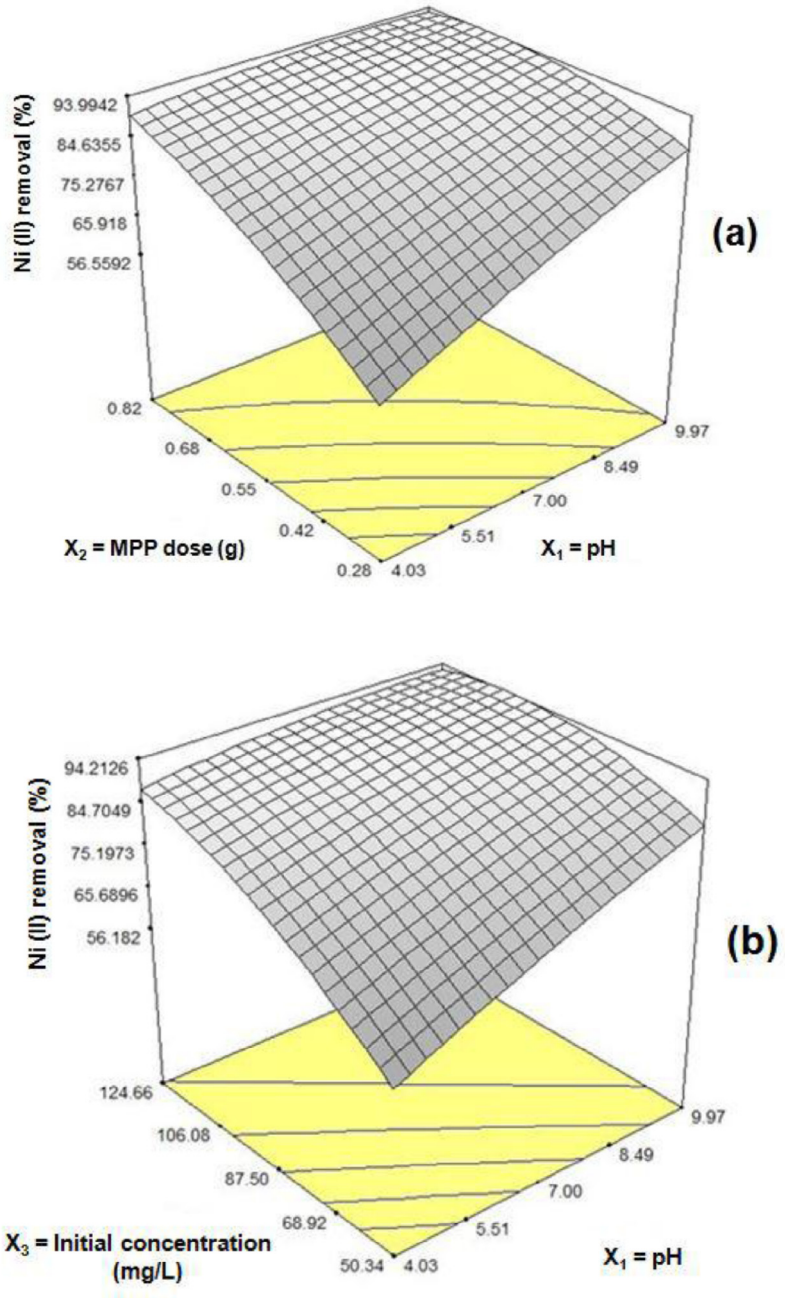


**Fig. 2 – Three-dimensional response surface plot (a) demonstrating the effect of pH and MPP dose with initial concentration fixed at zero level ($C_o$ = 88 mg/L); three-dimensional response surface plot (b) demonstrating the effect of pH and initial concentration with MPP dose fixed at zero level (W = 0.6 g) for Ni (II).**

### 3.5. *Adsorption isotherm*

To select the best fitted model for the experimental data, chi square ($\chi^2$) was incorporated since correlation coefficient ($R^2$) may not justify the basis for selection of the best adsorption model because it only represents the fit between experimental data and linearized forms of the isotherm equations while chi square ($\chi^2$) represents the fit between the experimental and the predicted values of the adsorption capacity. The lower the $\chi^2$ value, the better the fit.

Table 4 summarizes all the constants; $R^2$ and $\chi^2$ values obtained from the isotherm models applied for the two metal ions adsorption on MPP. The $Q_a^0$ values obtained for Ni (II) and Cd (II) from the linear Langmuir plot (Fig. 4a) were 77.52 and 70.92 mg/g respectively. According to the fitting results listed in Table 4, Langmuir isotherm model appeared to be much more applicable than the Freundlich having the highest $R^2$ as well as lowest $\chi^2$ values. The fitness of the Langmuir model to the adsorption process connotes that the metal ion molecules from bulk solution were adsorbed on specific monolayer which is homogeneous in nature. As can also be seen from Table 4, all the $R_L$ values lie between 0 and 1 which confirms the adsorption processes to be favourable under the studied conditions. The n values obtained from the Freundlich plot (Fig. 4b) were

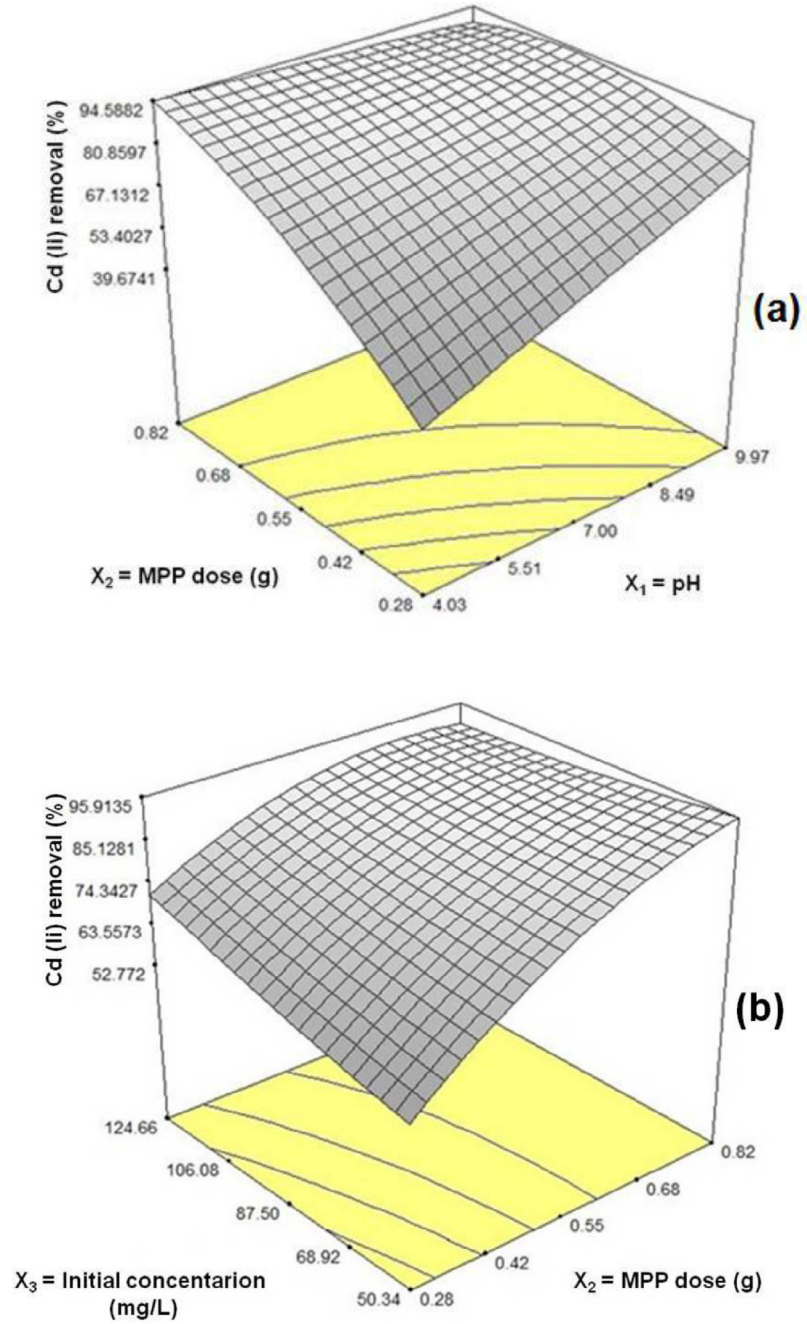


**Fig. 3 – Three-dimensional response surface plot (a) demonstrating the effect of pH and MPP dose with initial concentration fixed at zero level ($C_o$ = 88 mg/L); three-dimensional response surface plot (b) demonstrating the effect of MPP dose and initial concentration when pH was fixed (pH = 7) for Cd (II) removal.**

found to be greater than unity for the adsorbates, further indicating favourable adsorption conditions as well as physical adsorption processes for the two metal ions in aqueous solution.

The monolayer adsorption capacity ($Q_a^o$) values of 77.52 mg/g for Ni (II) and 70.92 mg/g for Cd (II) observed in this study compared well with some other adsorbents reported from literature such as 5.41 mg/g from dolomite powder (Mohammadi et al., 2015), 42.41 mg/g by modified chitosan (Cheng et al., 2014), 44.44 mg/g from *Bacillus laterosporus* MTC C 1628 (Kulkarni and Shetty, 2014) and 58.82 mg/g from tomato leaf powder (Gutha et al., 2015) for Ni (II) adsorption as well as 11.72 mg/g using olive stone activated carbon (Alslaibi et al., 2013), 1.62 mg/g obtained from dolomite powder (Mohammadi et al., 2015), 18.34 mg/g obtained using chemically modified onion skin (Agarry et al., 2015) and 85.47 mg/g from *B. laterosporus* MTC C 1628 (Kulkarni and Shetty, 2014) for the adsorption process of Cd (II).

### 3.6. *Kinetic studies*

The values of $q_{e\ cal}$, $k_1$, $R^2$ and $\chi^2$ obtained from the plot of pseudo-first-order and $q_{ecal}$, $k_2$, $R^2$ and $\chi^2$ obtained from the plot of pseudo-second-order kinetic models for the two metal ions

**Table 4 – Langmuir and Freundlich isotherm models for Ni (II) and Cd (II) adsorption onto MPP.**

| Isotherms | Parameters | Ni (II) | Cd (II) |
|---|---|---|---|
| Langmuir | $Q_a^0$ (mg/g) | 77.52 | 70.92 |
| | $K_L$ (L/mg) | 0.277 | 5.423 |
| | $R_L$ | 0.023 | 0.001 |
| | $R^2$ | 0.9658 | 0.9605 |
| | $\chi^2$ | 7.282 | 5.892 |
| Freundlich | $K_F$ (mg/g) (L/mg) | 16.151 | 18.595 |
| | n | 2.212 | 2.380 |
| | $R^2$ | 0.9466 | 0.9544 |
| | $\chi^2$ | 13.961 | 16.141 |

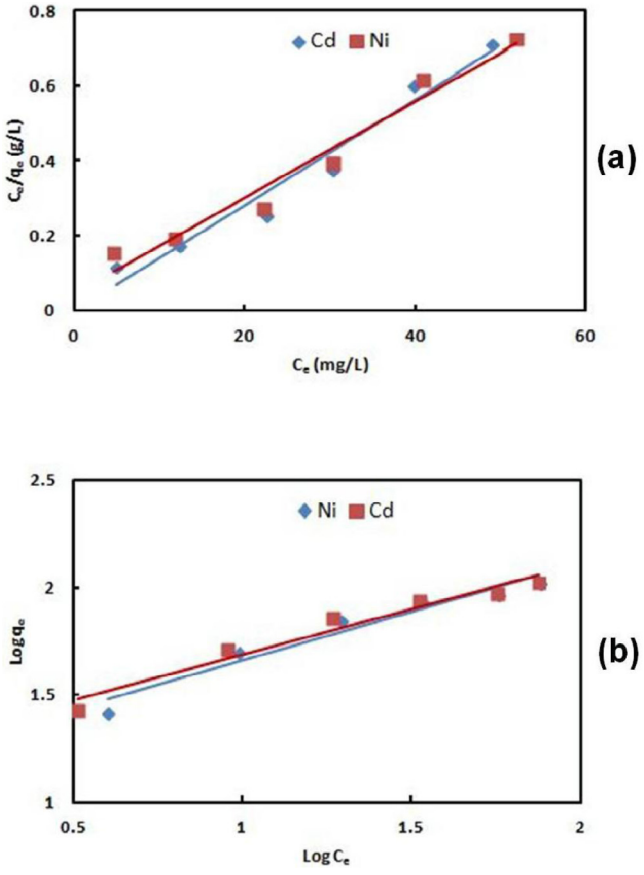


**Fig. 4 – (a) Langmuir isotherm and (b) Freundlich isotherm plot of Ni (II) and Cd (II) on MPP.**

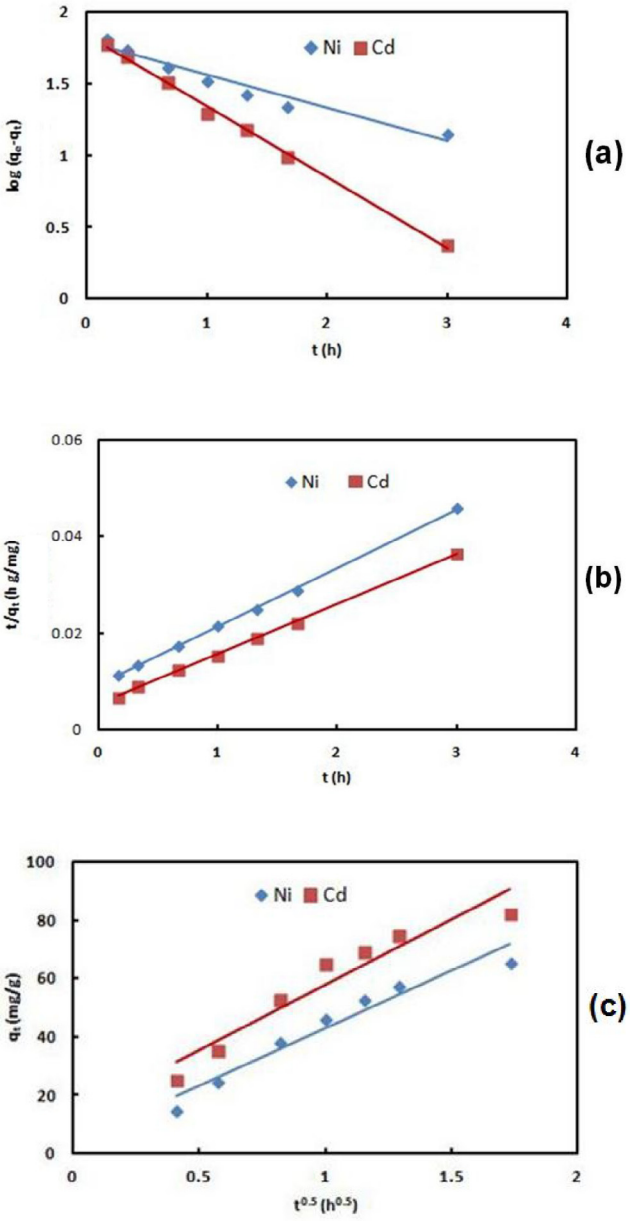


**Fig. 5 – (a) Pseudo-first-order kinetic, (b) pseudo-second-order kinetic, and (c) intraparticle diffusion plots for the adsorption of Ni (II) and Cd (II) on MPP.**

adsorption on the MPP were tabulated in Table 5. It can be seen that the $R^2$ values obtained from the pseudo-first-order model did not show a consistent trend and also the experimental $q_e$ ($q_{e\ exp}$) values did not agree with the calculated values ($q_{e\ cal}$) obtained from the linear plot (Fig. 5a). This shows that adsorption of the two metal ions onto MPP does not follow a pseudo first-order kinetic model. However, all the $R^2$ values obtained from the pseudo-second-order model were closer to unity with good agreement between the experimental and the calculated $q_e$ values obtained from the linear plot (Fig. 5b), further

**Table 5 – Pseudo-first-order, pseudo-second-order equation and intraparticle diffusion model constants for Ni (II) and Cd (II) adsorption onto MPP at 30 °C.**

| | $q_{e,exp}$ (mg/g) | Pseudo-first-order kinetic model | | | | Pseudo-second-order kinetic model | | | | Intraparticle diffusion model | | |
|---|---|---|---|---|---|---|---|---|---|---|---|---|
| | | $k_1$ (1/h) | $q_{e,cal}$ (mg/g) | $R^2$ | $\chi^2$ | $k_2$ (g/mg h) | $q_{e,cal}$ (mg/g) | $R^2$ | $\chi^2$ | $k_{p2}$ (mg/g $h^{1/2}$) | $C_2$ | $(R_2)^2$ |
| Ni (II) | 80.01 | 0.531 | 61.46 | 0.948 | 5.599 | 0.016 | 82.64 | 0.999 | 0.084 | 39.43 | 3.67 | 0.944 |
| Cd (II) | 84.66 | 1.135 | 68.56 | 0.997 | 3.781 | 0.020 | 97.08 | 0.999 | 1.589 | 44.87 | 13.13 | 0.919 |

confirming that the adsorption of the two metal ions on MPP fitted well into the pseudo-second-order model.

The values of $k_{pi}$, $C_i$ as well as the correlation coefficients, $R^2$, obtained from the intra particle plot (Fig. 5c) are also given in Table 5. Higher diffusion rate constant for Cd (II) can be observed from the table, indicating that the diffusion of Cd (II) was more rapid than that of Ni (II). It can also be observed from Fig. 5(c) that the linear lines of the plot for both adsorbates did not pass through the origin which suggested the presence of intraparticle diffusion but was not the only rate controlling step, some other rate controlling steps might be involved in the process (Garba et al., 2014).

## 4. Conclusion

Three adsorption parameters were optimized with the help of CCD, a subset of RSM for the adsorption of two heavy metal ions onto modified plantain peel (MPP) with their percentage removals ($Y_{Ni}$ and $Y_{Cd}$) as the analysis responses. Based on the results obtained, the three factors (pH, MPP dose and initial concentration) have varying impacts on the adsorption processes with MPP dose and initial concentration posing analogous influence on the Ni (II) adsorption while MPP had the greatest effect on Cd (II) adsorption. Highest removal percentage of the adsorbates was obtained at the optimum conditions of pH (4.36), MPP dose (0.82 g) and initial concentration (120 mg/L) with desirability of 1.00. Equilibrium and kinetic data analysed show Langmuir and pseudo-second-order to be the best fitted models respectively. Presence of intraparticle diffusion was also suggested to be involved in the adsorption process along with some other rate controlling steps.

## Acknowledgement

Zaharaddeen N. Garba would like to express his gratitude to the Tertiary Education Trust Fund and Ahmadu Bello University, Zaria, Nigeria for the study fellowship offered to him.

## REFERENCES

Agarry SE, Ogunleye OO, Ajani OA. Biosorptive removal of cadmium (II) ions from aqueous solution by chemically modified onion skin: batch equilibrium, kinetic and thermodynamic studies. Chem Eng Commun 2015;202:655–73.

Ahmad MA, Alrozi R. Optimization of preparation conditions for mangosteen peel-based activated carbons for the removal of Remazol Brilliant Blue R using response surface methodology. Chem Eng J 2010;165:883–90.

Alslaibi TM, Abustan I, Ahmad MA, Abu Foul A. Cadmium removal from aqueous solution using microwaved olive stone activated carbon. J Environ Chem Eng 2013;1:589–99.

Ashrafi SD, Kamani H, Mahvi AH. The optimization study of direct red 81 and Methylene blue adsorption on NaOH-modified rice husk. Desalination Water Treat 2014;57:738–46. doi:10.1080/19443994.2014.979329.

Cao J, Wu Y, Jin Y, Yilihan P, Huang W. Response surface methodology approach for optimization of the removal of chromium(VI) by NH2-MCM-41. J Taiwan Inst Chem Eng 2014;45:860–8.

Cheng Z, Ma W, Gao L, Gao Z, Wang R, Xu J, et al. Adsorption of nickel ions from seawater by modified chitosan. Desalination Water Treat 2014;52:5663–72.

Farghali AA, Bahgat M, Enaiet Allah A, Khedr MH. Adsorption of Pb(II) ions from aqueous solutions using copper oxide nanostructures. Beni-Suef Univ J Basic Appl Sci 2013;2:61–71.

Freundlich HMF. Over the adsorption in solution. J Phys Chem 1906;57:385–470.

Garba ZN, Afidah AR. Process optimization of $K_2C_2O_4$-activated carbon from Prosopis africana seed hulls using response surface methodology. J Anal Appl Pyrolysis 2014;107:306–12.

Garba ZN, Afidah AR. Optimization of activated carbon preparation conditions from Prosopis africana seed hulls for the removal of 2,4,6-Trichlorophenol from aqueous solution. Desalination Water Treat 2015;56:2879–89.

Garba ZN, Afidah AR, Hamza SA. Potential of Borassus aethiopum shells as precursor for activated carbon preparation by physico-chemical activation; optimization, equilibrium and kinetic studies. J Environ Chem Eng 2014;2:1423–33.

Garba ZN, Afidah AR, Bello BZ. Optimization of preparation conditions for activated carbon from Brachystegia eurycoma seed hulls: a new precursor using central composite design. J Environ Chem Eng 2015a;3:2892–9.

Garba ZN, Shikin FBS, Afidah AR. Valuation of activated carbon from waste tea for the removal of a basic dye from aqueous solution. J Chem Eng Chem Res 2015b;2:623–33.

Garba ZN, Ubam S, Babando AA, Galadima A. Quantitative assessment of heavy metals from selected tea brands marketed in Zaria, Nigeria. J Phys Sci 2015c;26:43–51.

Gómez Pacheco CV, Rivera Utrilla J, Sánchez Polo M, López Peñalver JJ. Optimization of the preparation process of biological sludge adsorbents for application in water treatment. J Hazard Mater 2012;217:76–84.

Gutha Y, Munagapati VS, Naushad N, Abburi K. Removal of Ni(II) from aqueous solution by Lycopersicum esculentum (Tomato) leaf powder as a low-cost biosorbent. Desalination Water Treat 2015;54:200–8.

Ho Y-S, Mckay G. Sorption of dye from aqueous solution by peat. Chem Eng J 1998;70:115–24.

Khavidaki HD, Aghaie H. Adsorption of thallium(I) ions using eucalyptus leaves powder. Clean (Weinh) 2013;41:673–9.

Kobya M, Demirbas E, Senturk E, Ince M. Adsorption of heavy metal ions from aqueous solutions by activated carbon prepared from apricot stone. Bioresour Technol 2005;96:1518–21.

Krishnan KA, Sreejalekshmi KG, Baiju RS. Nickel(II) adsorption onto biomass based activated carbon obtained from sugarcane bagasse pith. Bioresour Technol 2011;102:10239–47.

Kula I, Ugurlu M, Karaoglu H, Celik A. Adsorption of Cd (II) ions from aqueous solutions using activated carbon prepared from olive stone by $ZnCl_2$ activation. Bioresour Technol 2008;99:492–501.

Kulkarni RM, Shetty KV, Srinikethan G. Cadmium (II) and nickel (II) biosorption by Bacillus laterosporus (MTCC1628). J Taiwan Inst Chem Eng 2014;45:1628–35.

Lagergren S, Svenska BK. On the theory of so-called adsorption of dissolved substances. Royal Swed Acad Sci Doc 1898;24:1–13.

Langmuir I. The constitution and fundamental properties of solids and liquids. Part I. Solids. J Am Chem Soc 1916;38:2221–95.

Martins AC, Pezoti O, Cazetta AL, Bedin KC, Yamazaki DAS, Bandoch GFG, et al. Removal of tetracycline by NaOH-activated carbon produced from macadamia nut shells:

kinetic and equilibrium studies. Chem Eng J 2015;260:291–9.
Mekatel E, Amokrane S, Aid A, Nibou D, Trari M. Adsorption of methyl orange on nanoparticles of a synthetic zeolite NaA/CuO. C R Chim 2015;18:336–44.
Mohammadi M, Ghaemi A, Torab-Mostaedi M, Asadollahzadeh M, Hemmati A. Adsorption of cadmium (II) and nickel (II) on dolomite powder. Desalination Water Treat 2015;53:149–57.
Mohan D, Singh KP, Sing VK. Waste water treatment using low-cost activated carbons derived from agricultural byproducts – a case study. J Hazard Mater 2008;152:1045–53.
Mondal S, Sinha K, Aikat K, Halder G. Adsorption thermodynamics and kinetics of ranitidine hydrochloride onto superheated steam activated carbon derived from mung seed husk. J Environ Chem Eng 2015;3:187–95.
Ozdes D, Gundogdu A, Kemer B, Duran C, Senturk HB, Soylak M. Removal of Pb(II) ions from aqueous solution by a waste mud from copper mine industry: equilibrium, kinetic and thermodynamic study. J Hazard Mater 2009;166:1480–7.
Sadaf S, Bhatti HN, Nausheen S, Amin M. Removal of Cr(VI) from wastewater using acid-washed zero-valent iron catalyzed by polyoxometalate under acid conditions: efficacy, reaction mechanism and influencing factors. J Taiwan Inst Chem Eng 2015;47:160–70.
Sahu JN, Acharya J, Meikap BC. Optimization of production conditions for activated carbons from Tamarind wood by zinc chloride using response surface methodology. Bioresour Technol 2010;101:1974–82.
Serencam H, Gundogdu A, Uygur Y, Kemer B, Bulut VN, Duran C, et al. Removal of cadmium from aqueous solution by Nordmann fir (Abies nordmanniana (Stev.) Spach. Subsp. nordmanniana) leaves. Bioresour Technol 2008;99:1992–2000.
Shirzad-Siboni M, Khataee A, Hassani A, Karaca S. Preparation, characterization and application of a CTAB-modified nanoclay for the adsorption of an herbicide from aqueous solutions: kinetic and equilibrium studies. C R Chim 2015;18:204–14.
Subbaiah MV, Yuvaraja G, Vijaya Y, Krishnaiah A. Equilibrium, kinetic and thermodynamic studies on biosorption of Pb(II) and Cd(II) from aqueous solution by fungus (Trametes versicolor) biomass. J Taiwan Inst Chem Eng 2011;42:965–71.
Tan IAW, Ahmad AL, Hameed BH. Adsorption isotherms, kinetics, thermodynamics and desorption studies of 2,4,6-trichlorophenol on oil palm empty fruit bunch-based activated carbon. J Hazard Mater 2009;164:473–82.
Tsai WT, Chang CY, Lee SL. A low cost adsorbent from agricultural waste corn cob by zinc chloride activation. Bioresour Technol 1998;64:211–17.
Tuzen M, Sari A, Mendil D, Soylak M. Biosorptive removal of mercury(II) from aqueous solution using lichen (Xanthoparmelia conspersa) biomass: kinetic and equilibrium studies. J Hazard Mater 2009;169:263–70.
Verlicchi P, Galletti A, Petrovic M, Barcelo' D. Hospital effluents as a source of emerging pollutants: an overview of micropollutants and sustainable treatment options. J Hydrol (Amst) 2010;389:416–28.
Weber WJ, Morris JC. Kinetics of adsorption on carbon from solution. J Sanit Eng Div 1963;89:375–93.